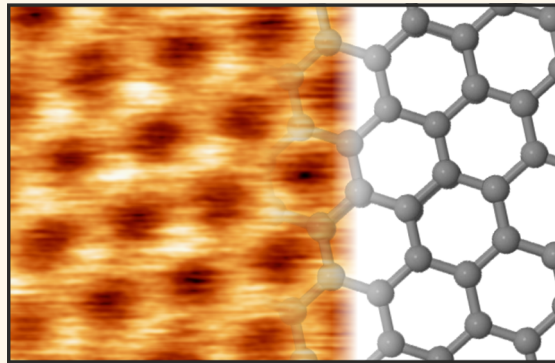


# Atomically Resolved Graphitic Surfaces in Air by Atomic Force Microscopy

Daniel S. Wastl,\* Alfred J. Weymouth, and Franz J. Giessibl

Institute of Experimental and Applied Physics, University of Regensburg, Universitätsstrasse 31, 93053 Regensburg, Germany

**ABSTRACT** Imaging at the atomic scale using atomic force microscopy in biocompatible environments is an ongoing challenge. We demonstrate atomic resolution of graphite and hydrogen-intercalated graphene on SiC in air. The main challenges arise from the overall surface cleanliness and the water layers which form on almost all surfaces. To further investigate the influence of the water layers, we compare data taken with a hydrophilic bulk-silicon tip to a hydrophobic bulk-sapphire tip. While atomic resolution can be achieved with both tip materials at moderate interaction forces, there are strong differences in force *versus* distance spectra which relate to the water layers on the tips and samples. Imaging at very low tip–sample interaction forces results in the observation of large terraces of a naturally occurring stripe structure on the hydrogen-intercalated graphene. This structure has been previously reported on graphitic surfaces that are not covered with disordered adsorbates in ambient conditions (*i.e.*, on graphite and bilayer graphene on SiC, but not on monolayer graphene on SiC). Both these observations indicate that hydrogen-intercalated graphene is close to an ideal graphene sample in ambient environments.



**KEYWORDS:** atomic resolution · air · graphene · graphitic surfaces · atomic force microscopy · ambient conditions · qPlus sensor

To understand atomic and molecular structures in biocompatible environments, tools for sensing down to the atomic and intermolecular scale in ambient conditions are needed.<sup>1–3</sup> One method to achieve this high resolution is atomic force microscopy,<sup>4–6</sup> where the highest spatial resolution is realized in ultrahigh vacuum. While imaging down to the atomic scale is possible in liquid<sup>7–9</sup> and ambient conditions,<sup>10</sup> the vaguely defined surface contamination films present in these environments are an ongoing challenge.

In 1995, it was shown that force microscopy could achieve atomic resolution of the Si(111)-7  $\times$  7 surface.<sup>6</sup> While the 7  $\times$  7 surface is an archetypical surface for scanning probe experiments, its adatoms with a spacing of 770 pm are much wider apart than atoms on other surfaces. After Si was atomically resolved, it was not until 2003 that the AFM was finally able to resolve each atom on a graphite surface.<sup>11</sup> Those eight years were not for lack of trying, but rather because of the close spacing of atoms in graphitic surfaces, which is only 142 pm. The simultaneous measurement of tunneling

currents and forces demonstrated the ability of force microscopy to resolve finer details than its predecessor, as tunneling microscopy generally only resolves every second atom of the surface. Resolving the graphite surface required data collection at low temperature and in ultrahigh vacuum (UHV). At low temperatures, the drift is decreased, allowing for measurements that demand low bandwidth. In UHV, the long-range forces are usually limited to electrostatic and van der Waals forces. Of course, many biological samples strongly rely upon their environment and are not suitable for studies in UHV or low temperatures. Not only does this require operation near room temperature, but the presence of any liquid, especially water, can complicate the system as a whole. Ignoring hydrodynamic forces,<sup>12</sup> the complications arise mainly because of two effects: The dipole moment of the water molecule and the naturally occurring OH<sup>–</sup> and H<sub>3</sub>O<sup>+</sup> ions. It is common that at interfaces one ionic species will be favored over the other and form a layer, attracting the second to form a complementary layer, known as an electric double

\* Address correspondence to daniel.wastl@physik.uni-regensburg.de.

Received for review March 5, 2014 and accepted April 18, 2014.

Published online April 18, 2014  
10.1021/nn501696q

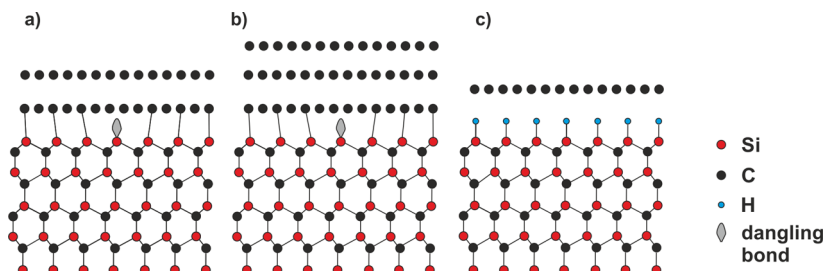


**Figure 1.** Model of epitaxial graphene on SiC(0001): (a) monolayer graphene and (b) bilayer graphene on SiC. The graphene sheet sits on top of an interface layer bound to the SiC substrate. (c) Hydrogen intercalated graphene on 6H-SiC(0001) is separated from the SiC substrate by a H layer.

layer. In a controlled liquid environment, these effects can be reduced or optimized by careful combination of the tip–sample–liquid (solution) system.<sup>12</sup>

Recently, we reported atomic imaging of KBr under ambient conditions by frequency-modulation atomic force microscopy (FM–AFM).<sup>10</sup> This is a very unique system in which the ionic species dissolve into the water layer, effectively decreasing the electrostatic effects. We acquired images in which one of the two ionic species (spaced by 466 pm) can be seen, similar to images previously reported in UHV.<sup>13,14</sup> We used a sharp hydrophobic sapphire tip, which appeared to have no measurable water layers on the apex, and optimized the signal-to-noise ratio with respect to the oscillation amplitude ( $A$ ), a method we called Q-spectroscopy.

## RESULTS AND DISCUSSION

In this work, we investigate highly oriented pyrolytic graphite (HOPG) and hydrogen-intercalated graphene (also referred to as quasi-free-standing monolayer graphene<sup>15–17</sup>) on SiC(0001). Hydrogen-intercalated graphene differs from both monolayer and bilayer graphene on SiC by the hydrogen termination of the underlying substrate (Figure 1), a point we will return to later. Both the graphite and graphene surfaces are hydrophobic. HOPG has been studied with contact angle measurements,<sup>18–20</sup> with results varying from 83.0°<sup>18</sup> to 98.3°,<sup>19</sup> and all studies agreeing that it is hydrophobic in nature. For this paper, we therefore interpret a contact angle of 80° or higher to indicate that a material is hydrophobic. While we are not aware of contact-angle measurements published on H-intercalated graphene, we propose that it is hydrophobic, too, for the following two reasons. First, while bare SiC is hydrophilic with a contact angle of 69.3°, as soon as monolayer, bilayer, or a few layers graphene are grown on it, it becomes hydrophobic with contact angles of 92.5°, 91.9°, and 92.7°, respectively.<sup>20</sup> The hydrogenation of the polar interface layer is unlikely to lead to a hydrophilic character. Second, we observe a structure on the H-intercalated graphene that we understand to be formed by gas aggregation on a hydrophobic surface.

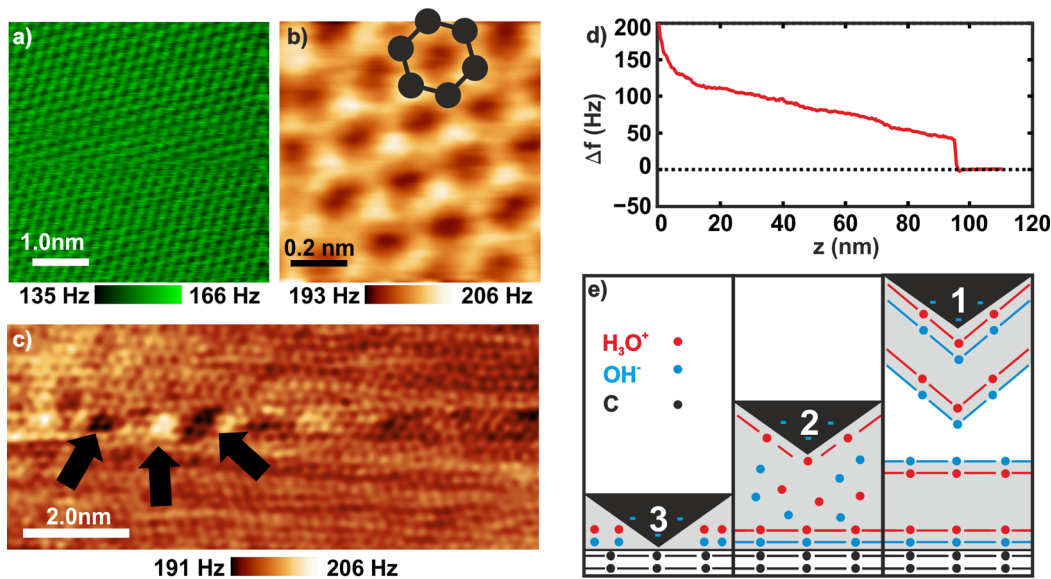
Our experiments are done in laboratory air with a relative humidity (RH) of 50–60%. We used both a hydrophobic sapphire tip and a hydrophilic bulk Si tip. The contact angle of a smoothed sapphire sample has been measured to be >80°.<sup>21</sup> The Si tip was made by a shard of a Si single crystal, which we expect is covered with silica and adsorbed water. Bare silica particles have been shown to be hydrophilic in nature as demonstrated by contact angles less than 10°.<sup>22</sup>

Figure 2a shows a frequency shift ( $\Delta f$ ) image of HOPG acquired in quasi-constant height with a Si tip. The hexagonal atomic lattice is clearly observable. In Figure 2b, a higher-resolution image is shown, where the atoms and single bonds can clearly be seen.

Figure 2c displays atomic-sized defects in the graphite surface. These defects were probably caused by a folding fault in a subsurface layer. Not surprisingly, we did not observe single-atom defects, as the creation of these on graphitic surfaces usually requires sputtering.

Shortly after imaging, we acquired a  $\Delta f$  versus tip–sample distance ( $z$ ) spectrum (Figure 2d). The spectrum shows three different features: (1) an onset of a long-range repulsion at 100 nm which leads to a very steep increase in the force gradient over a range of only a few nanometers, (2) an almost linear increase of  $\Delta f$  with decreasing distance that spans tens of nanometers, and (3) a strong repulsive interaction that is observable only at very small tip sample distances.

To explain this, we propose the following model (see Figure 2e): (1) At large tip–sample distances, the water layers on the tip and sample are not in contact but still interact. Water–gas interfaces are negatively charged due to the accumulation of  $\text{OH}^-$  ions, over a wide range of pH conditions.<sup>23,24</sup> The water–gas interface on the Si tip and graphite surface are therefore both negatively charged and repulsive. (2) At intermediate distances, the water layer on the sample and the tip are in contact. The dominant processes in this region are quite different because the interaction is no longer dominated by the electrostatic repulsion of the surface of two separate water layers. Many different effects come into play here, including the attractive meniscus formation, hydrodynamic forces caused by the moving tip, and the interaction between the surface electric



**Figure 2.** FM-AFM measurements on HOPG and model of silicon tip sample system. (a), (b)  $\Delta f$  images of HOPG: (a) atomic resolution of HOPG,  $\Delta f = 150$  Hz,  $A = 200$  pm; (b) high-resolution  $\Delta f$  image,  $\Delta f = 200$  Hz,  $A = 380$  p; (c)  $\Delta f$  images of atomic-sized defects in HOPG surface, with defects marked by arrows,  $\Delta f = 200$  Hz,  $A = 350$  pm; (d)  $\Delta f$  versus  $z$  spectrum on HOPG, the three different  $z$ -dependent states are marked observable; (e) model of the silicon tip and graphitic sample: (1) no direct contact between water layers; (2) water layers are in contact; (3) atomic resolution.

double layers. It was shown that on a silica surface in water, the solid–liquid interface charges due to deprotonated silanol groups<sup>25,26</sup> and positive counterions ( $\text{H}_3\text{O}^+$ ) are attracted by the surface potential.<sup>25</sup> Furthermore, the presence of the liquid layer can lead to repulsive van der Waals forces (Casimir–Lifshitz force).<sup>27</sup> This is therefore a very complicated regime which is observable in the force spectrum with this relatively flat, hydrophilic tip. (3) At small tip–sample distances, the tip is sensitive to short-range forces and atomic resolution can be achieved. At low temperature in UHV, investigations of graphitic surfaces<sup>28</sup> and molecules<sup>4,29</sup> have concluded that Pauli repulsion is responsible for these short-range interactions. We propose the same interaction in ambient conditions because we find similar image contrast, with the atoms appearing repulsive.

After imaging the HOPG surface, we imaged hydrogen-intercalated graphene on SiC(0001) with the same silicon tip. Again, we can observe atomic resolution of the lattice (Figure 3a). A  $\Delta f$  versus  $z$  spectrum (Figure 3b) appeared very similar to the one on graphite, indicating similar physical processes in the three regimes.

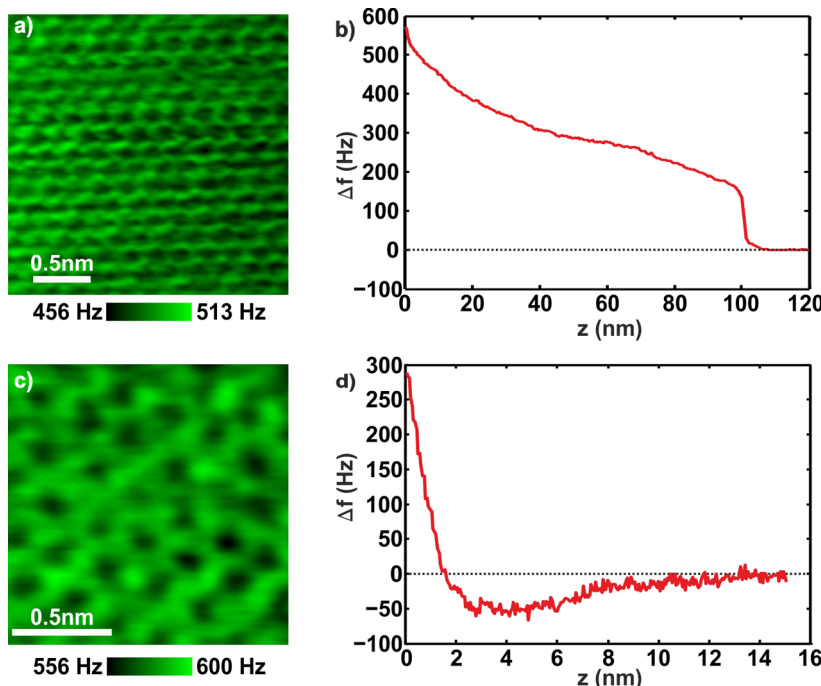
For the comparison of hydrophobic and hydrophilic tip materials, we measured with bulk sapphire tips ( $\text{Al}_2\text{O}_3$ ). High wear resistance, chemical inertness, and high hydrophobicity make sapphire a nearly ideal tip material.

Figure 3c shows an image of the graphene surface with the sapphire tip. The  $\Delta f$  versus  $z$  spectrum (Figure 3d) shows an attractive interaction beginning from 12 nm distance which changes into short-range repulsion at a distance of 2 nm from the surface. We relate this to the absence or reduction of water layers on the sapphire tip.

While the atomic resolution with the sapphire and silicon tips are similar (Figure 3a,c), the  $\Delta f$  versus  $z$  spectra (Figure 3b,d) are vastly different. Atomic resolution requires a tip apex that is the same size or smaller than the lateral features to resolve. Therefore, both a Si tip and a sapphire tip, ending in a single atom, are capable of producing similar images with atomic resolution. The differences in spectra, however, are due primarily to the interaction of the macroscopic tip with the water layer. This is a function of many parameters including the sharpness of the tip and how hydrophilic or hydrophobic the material is. The Si tip spectrum shows interactions over a range of 100 nm from the point of atomic resolution, while the sapphire tip which shows these interactions only over a range of 12 nm. This indicates that the Si tip is not as sharp as the sapphire tip.

We found it easier to achieve atomic resolution on graphene with Si tips. Our hypothesis for this is that the inert behavior of sapphire and the hardness of the crystal makes it hard to form the tip apex, whereas the Si tip can be changed easier by gentle surface pokes until atomic resolution is achieved. For Si tips we found that once a good tip apex was formed, it was as stable as the sapphire tips, and one could image without discontinuities or strong tip changes while achieving atomic resolution in experiments. The oxide seems very robust and wear resistant while resolving atoms over days even when switching from one sample to the other.

Using the sapphire tip, we explored larger surface features at smaller tip–sample interactions (Figure 4). We observe large flat terraces where only a few



**Figure 3.** FM-AFM measurements on hydrogen-intercalated graphene on 6H-SiC(0001): (a) atomic resolution  $\Delta f$  image with silicon tip; (b)  $\Delta f$  versus  $z$  spectrum with silicon tip  $\Delta f = 480$  Hz,  $A = 280$  pm. The three different distance dependent states between  $\Delta f$  and sample are observable. (c)  $\Delta f$  image with sapphire tip showing atomic resolution,  $\Delta f = 580$  Hz,  $A = 200$  pm; (d)  $\Delta f$  versus  $z$  spectrum with sapphire tip.

adsorbates are present. In contrast, the step edges are highly covered with adsorbates, in agreement with other experimental and theoretical data.<sup>30–32</sup> A closer look at the flat terraces revealed a naturally occurring stripe structure. The height of the stripe structure is 0.3–0.4 nm with a periodicity of ~4.2 nm.

The periodicity and height of the stripe structure are equal to reported structures on graphite<sup>33</sup> and bilayer graphene<sup>34</sup> and are proposed to be formed by the water-mediated adsorption of nitrogen on hydrophobic surfaces.<sup>33</sup> This phenomenon of gas enrichment (in this case N<sub>2</sub>) on a hydrophobic solid–liquid interface was theoretically predicted in molecular dynamic simulations.<sup>35</sup> As reported previously, the stripe structure can easily be destroyed by the tip.<sup>33</sup> While we can image these stripes, when imaging with atomic resolution we must be penetrating through this fragile stripe structure.

In recent work, we looked at a sample with both non-intercalated bilayer and monolayer graphene parts of the surface on SiC(0001).<sup>34</sup> The monolayer graphene was covered with disordered adsorbates, whereas the stripe structure could be observed on the bilayer area. Similarly, a higher reactivity has been found for monolayer graphene compared to thicker graphene in oxidation<sup>36,37</sup> and electron-transfer chemistry experiments.<sup>38</sup> It was observed that monolayer graphene is up to 10 times more chemically reactive than few-layer graphene in certain cases.<sup>38</sup> We proposed that as the monolayer graphene was covered by disordered adsorbates they precluded the formation of the

ordered stripe structure. Two effects that can influence the presence of these additional disordered adsorbates are substrate effects (including dangling bonds) and curvature.

Experiments and theoretical models show that both binding energy and adsorption barriers are tunable by controlling the local curvature of the graphene lattice.<sup>30–32</sup> Corrugation-induced reactivity was proposed on monolayer graphene.<sup>34,39</sup> It was shown that due to the spacing to the polar interface layer, the bilayer graphene is less corrugated<sup>40,41</sup> than monolayer graphene.

Raffee *et al.* showed that substrate properties can be important for the properties of the grapheme-coated surface and may mediate substrate properties to the surface.<sup>42</sup> Recently, Shih *et al.* showed that substrate effects can be effectively shielded<sup>43</sup> by increasing the distance between graphene and the substrate.

Substrate-induced charges and corrugation of graphene are still under discussion regarding their influence on the reactivity of graphene.<sup>36–38,44,45</sup> However, the presence of the stripe structure over such a large area of the hydrogen-intercalated graphene is a strong indication that the surface is flat and does not attract unwanted adsorbates. We propose that this is another reason that we were able to achieve atomic resolution on this surface, as we were able to scan on very clean terraces. Moreover, it shows that hydrogen-intercalated graphene is a near-ideal graphene surface in ambient conditions.

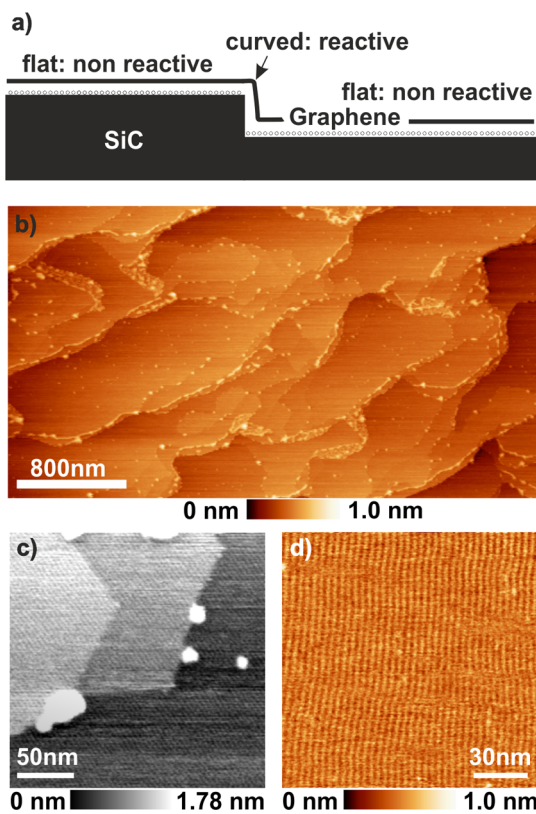


**Figure 4.** Hydrogen-intercalated epitaxially grown graphene on SiC(0001) with sapphire tip: (a) model of a step, where the graphene lies over a step like a carpet; (b) large scale overview; (c) stripe pattern which covers complete terraces of the graphene surface is observed; (d) high-resolution image of the stripes. The height of the stripe structure is 0.3–0.4 nm with a periodicity of  $\sim 4.2$  nm. Scan parameters  $\Delta f = 4.0$  Hz,  $A = 140$  pm.

## CONCLUSION

We imaged graphite with a hydrophilic Si tip and were able to achieve atomic resolution. The spectrum over this surface revealed measurable interaction further than 100 nm from the tip–sample imaging distance required for atomic resolution.

We imaged hydrogen-intercalated graphene with the Si tip and with a hydrophobic bulk-sapphire tip. The spectra showed clearly the difference between a tip covered by water layers and one without. Therefore,

when scanning with a bulk-silicon tip, which is very common in AFM, one needs to be very careful when interpreting surface *versus* tip features in the spectra.

We achieved atomic resolution with both tip materials. This was an outstanding result for us, as we have struggled for a long time to achieve atomic resolution on monolayer graphene. Comparing these data with our previous observations,<sup>34</sup> there is a clear difference between hydrogen intercalated and nonintercalated graphene on 6H-SiC(0001). Whereas the monolayer graphene was covered with disordered adsorbates,<sup>34</sup> the hydrogen-intercalated graphene remained clean. Fitting with our understanding of graphitic surfaces in ambient conditions, because the surface stayed free of disordered adsorbates, we were able to observe a stripe structure.

Our previous observations also showed this stripe structure on small bilayer regions of graphene. What makes monolayer graphene different from both bilayer and hydrogen-intercalated graphene is its proximity to the interface layer. We propose that the cleanliness of the hydrogen-intercalated graphene is due to the saturation of the underlying substrate, and that hydrogen-intercalated graphene is flatter and less attractive to disordered adsorbates than monolayer graphene. Transport measurements have also shown hydrogen-intercalated graphene to have a much higher mobility than monolayer graphene that is relatively constant with temperature.<sup>48</sup> Therefore, we propose that hydrogen-intercalated graphene is a strong candidate for manufacturing devices usable under ambient conditions and the stripe structure to be an indicator for low reactive graphene-coated surfaces.

A key feature in our setup is the qPlus<sup>10,46,47</sup> sensor and the small-amplitude operation at high  $Q$  values that it allows for. In contrast to standard AFMs, where cantilever stiffnesses range from 0.1 to 10 N/m, the qPlus sensor used here has a stiffness of 1280 N/m. We can controllably oscillate with amplitudes below 100 pm in a range of environments, from tens of nanometers thick water layers to almost none. It is easy to select the tip material, as the tip is simply glued to the end of the cantilever.

## MATERIALS AND METHODS

**Sample.** The HOPG crystals under study were purchased from Mateck GmbH and prepared by cleaving with adhesive tape in air. The hydrogen-intercalated epitaxially grown graphene on SiC(0001)<sup>15,17</sup> was provided by the group of Seyller.

**Quartz Cantilever AFM.** The AFM experiments were performed on a home-built qPlus ambient AFM,<sup>10,34</sup> operated by a Nanonis Control System with an OC4 PLL from SPECS GmbH. We used custom-designed qPlus<sup>10,46,47</sup> sensors that are manufactured similar as quartz tuning-forks. The sensors have a characteristic resonance frequency of  $f_0 = 32768$  Hz and a stiffness  $k = 1280$  N/m. The qPlus Sensors were equipped with silicon or sapphire tips, made by splintering bulk crystals. Sensor parameters: Figure 2

and Figure 3a,b:  $f_0 = 29858$  Hz,  $Q_{\text{air}} = 2432$ , bulk silicon tip; Figure 3c,d:  $f_0 = 30957$  Hz,  $Q_{\text{air}} = 2455$ , bulk sapphire tip. The amplitudes are optimized by Q-spectroscopy.

**Q-Spectroscopy.** The imaging amplitude  $A$  was optimized by a method described in detail in a previous publication.<sup>10</sup> Drive amplitude *versus* amplitude spectra are taken close to the sample and far away in air. Using these spectra, one can calculate the energy loss per oscillation cycle. From that, the effective  $Q$  value for the actual tip sample configuration can be determined. Here we note that on HOPG crystals effective  $Q$  values of up to 800 have been achieved.

**Quasi-constant Height Imaging.** AFM images in Figures 2 and shown in this manuscript were taken in quasi-constant height mode; *i.e.*, the feedback controller was set to a very low gain to

merely correct for thermal drift and essentially enable constant-height scanning.

**Tip Treatment.** If it was not possible to get atomic resolution upon the first approach to the sample, we changed the tip apex by performing light ( $\sim 1$ – $4$  nm) surface pokes on the graphene-coated SiC(0001). Surface contaminants were avoided to avoid tip contaminations. This worked quite well for Si tips, as Si is softer than SiC. Sapphire tips could be modified by poking into a sapphire substrate.

**Conflict of Interest:** The authors declare no competing financial interest.

**Acknowledgment.** We thank Thomas Seyller and Florian Speck for the graphene samples and Thomas Hofmann and Michael Lemberger for discussions. Financial support from the Deutsche Forschungsgemeinschaft (GRK 1570, SFB 689) is gratefully acknowledged.

## REFERENCES AND NOTES

1. Fukuma, T.; Kobayashi, K.; Matsushige, K.; Yamada, H. True Molecular Resolution in Liquid by Frequency-Modulation Atomic Force Microscopy. *Appl. Phys. Lett.* **2005**, *86*, 193108.
2. Schreiber, M.; Eckardt, M.; Klassen, S.; Adam, H.; Nalbach, M.; Greifenstein, L.; Kling, F.; Kittelmann, M.; Bechstein, R.; Kühnle, A. How Deprotonation Changes Molecular Self-Assembly – an AFM Study in Liquid Environment. *Soft Matter* **2013**, *9*, 7145.
3. Yoo, P. J.; Nam, K. T.; Qi, J.; Lee, S.-K.; Park, J.; Belcher, A. M.; Hammond, P. T. Spontaneous Assembly of Viruses on Multilayered Polymer Surfaces. *Nat. Mater.* **2006**, *5*, 234–240.
4. Gross, L.; Mohn, F.; Moll, N.; Liljeroth, P.; Meyer, G. The Chemical Structure of a Molecule Resolved by Atomic Force Microscopy. *Science* **2009**, *325*, 1110–1114.
5. Binnig, G.; Quate, C. F.; Gerber, Ch. Atomic Force Microscope. *Phys. Rev. Lett.* **1986**, *56*, 930–933.
6. Giessibl, F. J. Atomic Resolution of the Silicon (111)-(7 $\times$ 7) Surface by Atomic Force Microscopy. *Science* **1995**, *267*, 68–71.
7. Fukuma, T.; Kobayashi, K.; Matsushige, K.; Yamada, H. True Atomic Resolution in Liquid by Frequency-Modulation Atomic Force Microscopy. *Appl. Phys. Lett.* **2005**, *87*, 034101.
8. Ichii, T.; Fujimura, M.; Negami, M.; Murase, K.; Sugimura, H. Frequency Modulation Atomic Force Microscopy in Ionic Liquid Using Quartz Tuning Fork Sensors. *Jpn. J. Appl. Phys.* **2012**, *51*, 08KB08.
9. Rode, S.; Oyabu, N.; Kobayashi, K.; Yamada, H.; Kühnle, A. True Atomic-Resolution Imaging of (1014) Calcite in Aqueous Solution by Frequency Modulation Atomic Force Microscopy. *Langmuir* **2009**, *25*, 2850–2853.
10. Wastl, D. S.; Weymouth, A. J.; Giessibl, F. J. Optimizing Atomic Resolution of Force Microscopy in Ambient Conditions. *Phys. Rev. B* **2013**, *87*, 245415.
11. Hembacher, S.; Giessibl, F. J.; Mannhart, J.; Quate, C. F. Revealing the Hidden Atom in Graphite by Low-Temperature Atomic Force Microscopy. *Proc. Natl. Acad. Sci. U.S.A.* **2003**, *100*, 12539–12542.
12. Butt, H.-J.; Cappella, B.; Kappl, M. Force Measurements with the Atomic Force Microscope: Technique, Interpretation and Applications. *Surf. Sci. Rep.* **2005**, *59*, 1–152.
13. Meyer, E.; Heinzelmann, H.; Rudin, H.; Güntherodt, H.-J. Atomic Resolution on LiF (001) by Atomic Force Microscopy. *Z. Phys. B* **1990**, *79*, 3–4.
14. Meyer, G.; Amer, N. M. Optical-Beam-Deflection Atomic Force Microscopy: The NaCl (001) Surface. *Appl. Phys. Lett.* **1990**, *56*, 2100.
15. Speck, F.; Jobst, J.; Fromm, F.; Ostler, M.; Waldmann, D.; Hundhausen, M.; Weber, H. B.; Seyller, T. The Quasi-Free-Standing Nature of Graphene on H-Saturated SiC(0001). *Appl. Phys. Lett.* **2011**, *99*, 122106.
16. Watcharinyanon, S.; Virojanadara, C.; Osiecki, J. R.; Zakharov, a. a.; Yakimova, R.; Uhrberg, R. I. G.; Johansson, L. I. Hydrogen Intercalation of Graphene Grown on 6H-SiC(0001). *Surf. Sci.* **2011**, *605*, 1662–1668.
17. Riedl, C.; Coletti, C.; Iwasaki, T.; Zakharov, A. A.; Starke, U. Quasi-Free-Standing Epitaxial Graphene on SiC Obtained by Hydrogen Intercalation. *Phys. Rev. Lett.* **2009**, *103*, 246804.
18. Zhang, Y.; Lu, R.; Liu, Q.; Song, Y.; Jiang, L.; Liu, Y.; Zhao, Y.; Li, T. J. Influence of Surface Hydrophobicity of Substrates on the Self-Organization of Chiral Molecule. *Thin Solid Films* **2003**, *437*, 150–154.
19. Wang, S.; Zhang, Y.; Abidi, N.; Cabrales, L. Wettability and Surface Free Energy of Graphene Films. *Langmuir* **2009**, *25*, 11078–11081.
20. Shin, Y. J.; Wang, Y.; Huang, H.; Kalon, G.; Wee, A. T. S.; Shen, Z.; Bhatia, C. S.; Yang, H. Surface-Energy Engineering of Graphene. *Langmuir* **2010**, *26*, 3798–3802.
21. Gorb, E. V.; Hosoda, N.; Miksch, C.; Gorb, S. N. Slippery Pores: Anti-Adhesive Effect of Nanoporous Substrates on the Beetle Attachment System. *J. R. Soc. Interface* **2010**, *7*, 1571–1579.
22. Kulkarni, S. A.; Ogale, S. B.; Vijayamohanan, K. P. Tuning the Hydrophobic Properties of Silica Particles by Surface Silanization Using Mixed Self-Assembled Monolayers. *J. Colloid Interface Sci.* **2008**, *318*, 372–379.
23. Takahashi, M. Zeta Potential of Microbubbles in Aqueous Solutions: Electrical Properties of the Gas–Water Interface. *J. Phys. Chem. B* **2005**, *109*, 21858–21864.
24. Beattie, J. K.; Djerdjev, A. M.; Warr, G. G. The Surface of Neat Water Is Basic. *Faraday Discuss.* **2009**, *141*, 31.
25. O'Reilly, J. P.; Butts, C. P.; L'Anson, I. A.; Shaw, A. M. Interfacial pH at an Isolated Silica–Water Surface. *J. Am. Chem. Soc.* **2005**, *127*, 1632–1633.
26. Iler, R. K. *The Chemistry of Silica: Solubility, Polymerization, Colloid and Surface Properties and Biochemistry of Silica*; Wiley & Sons: New York, 1979; pp 623–729.
27. Munday, J. N.; Capasso, F.; Parsegian, V. A. Measured Long-Range Repulsive Casimir–Lifshitz Forces. *Nature* **2009**, *457*, 170–173.
28. Hembacher, S.; Giessibl, F. J.; Mannhart, J. Force Microscopy with Light-Atom Probes. *Science* **2004**, *305*, 380–383.
29. Gross, L.; Mohn, F.; Moll, N.; Meyer, G.; Ebel, R.; Abdel-Mageed, W. M.; Jaspars, M. Organic Structure Determination Using Atomic-Resolution Scanning Probe Microscopy. *Nat. Chem.* **2010**, *2*, 821–825.
30. Goler, S.; Coletti, C.; Tozzini, V.; Piazza, V.; Mashoff, T.; Beltram, F.; Pellegrini, V.; Heun, S. Influence of Graphene Curvature on Hydrogen Adsorption: Toward Hydrogen Storage Devices. *J. Phys. Chem. C* **2013**, *117*, 11506–11513.
31. Tozzini, V.; Pellegrini, V. Reversible Hydrogen Storage by Controlled Buckling of Graphene Layers. *J. Phys. Chem. C* **2011**, *115*, 25523–25528.
32. Boukhvalov, D. W.; Katsnelson, M. I. Enhancement of Chemical Activity in Corrugated Graphene. *J. Phys. Chem. C* **2009**, *113*, 14176–14178.
33. Lu, Y.-H.; Yang, C.-W.; Hwang, I.-S. Molecular Layer of Gaslike Domains at a Hydrophobic–Water Interface Observed by Frequency-Modulation Atomic Force Microscopy. *Langmuir* **2012**, *28*, 12691–12695.
34. Wastl, D. S.; Speck, F.; Wutscher, E.; Ostler, M.; Seyller, T.; Giessibl, F. J. Observation of 4 nm Pitch Stripe Domains Formed by Exposing Graphene to Ambient Air. *ACS Nano* **2013**, *7*, 10032–10037.
35. Dammer, S.; Lohse, D. Gas Enrichment at Liquid–Wall Interfaces. *Phys. Rev. Lett.* **2006**, *96*, 206101.
36. Liu, L.; Ryu, S.; Tomasik, M. R.; Stolyarova, E.; Jung, N.; Hybertsen, M. S.; Steigerwald, M. L.; Brus, L. E.; Flynn, G. W. Graphene Oxidation: Thickness-Dependent Etching and Strong Chemical Doping. *Nano Lett.* **2008**, *8*, 1965–1970.
37. Yamamoto, M.; Einstein, T. L.; Fuhrer, M. S.; Cullen, W. G. Charge Inhomogeneity Determines Oxidative Reactivity of Graphene on Substrates. *ACS Nano* **2012**, *6*, 8335–8341.

38. Sharma, R.; Baik, J. H.; Perera, C. J.; Strano, M. S. Anomalously Large Reactivity of Single Graphene Layers and Edges Toward Electron Transfer Chemistries. *Nano Lett.* **2010**, *10*, 398–405.

39. Speck, F.; Ostler, M.; Röhrl, J.; Emtsev, K. V.; Hundhausen, M.; Ley, L.; Seyller, T. Atomic Layer Deposited Aluminum Oxide Films on Graphite and Graphene Studied by XPS and AFM. *Phys. Status Solidi* **2010**, *7*, 398–401.

40. Mallet, P.; Varchon, F.; Naud, C.; Magaud, L.; Berger, C.; Veuillen, J.-Y. Electron States of Mono- and Bilayer Graphene on SiC Probed by Scanning-Tunneling Microscopy. *Phys. Rev. B* **2007**, *76*, 041403.

41. Lauffer, P.; Emtsev, K. V.; Graupner, R.; Seyller, T.; Ley, L. Atomic and Electronic Structure of Few-Layer Graphene on SiC(0001) Studied with Scanning Tunneling Microscopy and Spectroscopy. *Phys. Rev. B* **2008**, *77*, 155426.

42. Rafiee, J.; Mi, X.; Gullapalli, H.; Thomas, A. V.; Yavari, F.; Shi, Y.; Ajayan, P. M.; Koratkar, N. a. Wetting Transparency of Graphene. *Nat. Mater.* **2012**, *11*, 217–222.

43. Shih, C.-J.; Wang, Q. H.; Lin, S.; Park, K.-C.; Jin, Z.; Strano, M. S.; Blankschtein, D. Breakdown in the Wetting Transparency of Graphene. *Phys. Rev. Lett.* **2012**, *109*, 176101.

44. Wang, Q. H.; Jin, Z.; Kim, K. K.; Hilmer, A. J.; Paulus, G. L. C.; Shih, C.-J.; Ham, M.-H.; Sanchez-Yamagishi, J. D.; Watanabe, K.; Taniguchi, T.; et al. Understanding and Controlling the Substrate Effect on Graphene Electron-Transfer Chemistry via Reactivity Imprint Lithography. *Nat. Chem.* **2012**, *4*, 724–732.

45. Fan, X.; Nouchi, R.; Tanigaki, K. Effect of Charge Puddles and Ripples on the Chemical Reactivity of Single Layer Graphene Supported by SiO<sub>2</sub>/Si Substrate. *J. Phys. Chem. C* **2011**, *115*, 12960–12964.

46. Giessibl, F. J. Atomic Resolution on Si(111)-(7×7) by Non-contact Atomic Force Microscopy with a Force Sensor Based on a Quartz Tuning Fork. *Appl. Phys. Lett.* **2000**, *76*, 1470.

47. Schneiderbauer, M.; Wastl, D.; Giessibl, F. J. qPlus Magnetic Force Microscopy in Frequency-Modulation Mode with Millihertz Resolution. *Beilstein J. Nanotechnol.* **2012**, *3*, 174–178.

48. Speck, F.; Jobst, J.; Fromm, F.; Ostler, M.; Waldmann, D.; Hundhausen, M.; Weber, H. B.; Seyller, T. The Quasi-Free-Standing Nature of Graphene on H-Saturated SiC(0001). *Appl. Phys. Lett.* **2011**, *99*, 122106.